

STUDY OF THE HYDRODYNAMICS AND DISPERSE STRUCTURE OF A JET SPRAY  
BY THE METHOD OF LASER DIAGNOSIS

V. A. Borodulya, A. Zh. Greben'kov,  
V. I. Rubezhanskii, and I. V. Khodan

UDC 532.525.3+535.8

A study is made of the fine structure of the jet spray from a multiphase centrifugal nozzle using optical methods.

The use of contact methods and photography does not give a complete representation of flow hydrodynamics in empirical determinations of the gasdynamic characteristics of two-phase flows. Thus, contactless methods are being increasingly employed to study liquid atomization processes. One of the methods is the laser-Doppler method [1], which makes it possible to obtain quantitative information on the dynamic characteristics and disperse structure of multiphase flows [2, 3]. Also of definite interest are optical methods of visualization, which make it possible to obtain a clear qualitative picture of the processes: the distributions of particle concentrations in the flow and of particle dimensions, velocities, and paths.

Photographic recording of particles in scattered light (the laser "knife" method [4]) is best used to determine the general flow pattern in the macrorecording regime.

The present work uses the laser-Doppler and laser "knife" methods to determine the dynamic characteristics and disperse structure of a spray from a pneumatic nozzle, as well as the effect of an additionally introduced third component on these characteristics. We used the liquid spray obtained from the nozzle described in [5] as the object of our study.

The optical system for forming the laser "knife" included the radiation source (an LG-38 laser) and a telescope system. The latter included a lens with a focal length of 30 and 180 mm to increase the cross section of the laser beam to the required size and reduce its divergence angle. The telescope system also included a cylindrical lens which formed a plane-parallel beam.

The study [6] showed that the minimum particle size  $d$  that can be recorded by the above method is related to the resolving power of the optical system and the photographic material  $R_0 \geq 1/d_{\min}$ . The time of exposure should be  $\tau_n \leq R/V$ .

The condition for resolving individual particles, present in the flow in a concentration  $n_0$ , leads to limitation of the thickness  $t$  of the light beam. In recording without the superposition of the images of individual particles, the total number of particles  $N$  should be less than the ratio  $S/S_0$ , where  $S$  is the cross sectional area of the light "knife" in the field of view of the objective and  $S_0 = \pi R^2$  is the mean cross-sectional area of one particle. Then with a certain value of  $n_0$  the total number of particles is

$$N = n_0 t S \leq S / \pi R^2$$

and thus

$$t \leq \frac{1}{\pi R^2 n_0}.$$

In accordance with [5, 7] to obtain a good signal-to-noise ratio in measuring velocity by means of a laser-Doppler velocity meter (LDVM), particles of kaolin 1 to 5  $\mu\text{m}$  in diameter were introduced into the flow. It was shown in [8] that particles of this size follow a gas flow with a high degree of accuracy.

Figure 1 shows a diagram of a nozzle jet spray obtained by means of a laser knife. The structure of the spray is quite clear. The center region inside the jet constitutes the core

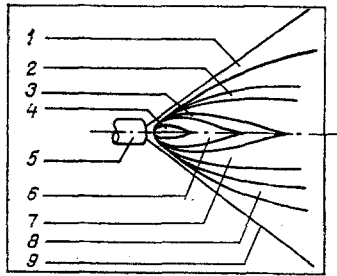


Fig. 1. Diagram of structure of jet spray: 1) zone of intensive mixing; 2) external boundary layer; 3) internal boundary layer; 4) core; 5) nozzle; 6) zone of constant velocity; 7) zone of high velocity; 8) transitional zone; 9) boundary of jet.

of the back flows enveloped by the carrier flow. The dimensions and shape of the back-flow core may change, depending on the nozzle characteristics and operating regime (geometric dimensions, ratios of air and liquid flow rates, pressure of the compressed air, etc.), but the core is always present, reminiscent of a flying drop in its shape. The length of the back-flow core  $l$  depends appreciably on the ratio of the flow rates of the compressed air  $G_a$  and the atomized liquid  $G_q$  and can be described by the empirical relation

$$l \sim \left( \frac{G_a}{G_q} \right)^{0.30} \quad (1)$$

Study of the structure of the surrounding flow in the vicinity of the core by means of LDVM showed that the flow has a nonuniform velocity distribution over its cross section and is bounded by two boundary layers: an "internal" layer surrounding the back-flow core, and an "external" layer at the periphery of the jet spray.

Table 1 presents values of the external "boundary" layer  $b_e$ , obtained experimentally, and  $b$ , calculated by the empirical formula [9]:

$$b = nr + b_n \quad (2)$$

The nonuniformity factor was determined from the Abramovich formula [10]:

$$n = 2 \int_0^1 \left( \frac{V_0}{V_{0m}} \right)^2 r dr \quad (3)$$

The degree of turbulence of the "external" boundary layer was 3%. With an increase in the distance from the axis, a zone of intensive mixing of the jet with the material of the submerged space was created, and the degree of turbulence reached 35%. Measurement of the velocity profile of the jet spray in the initial section at four stations  $X = 5, 10, 20,$  and  $30$  mm (Fig. 2a) and at greater distances (Fig. 2b and c) showed that air and particle velocities on the initial section and at the station  $X = 200$  mm or greater did not change substantially, while they decreased sharply within the range  $X = 40-200$  mm. It is interesting to note that on the initial section the maxima of axial and tangential velocity of the carrier (air) flow do not coincide, but their ratio, according to the experimental results

$$r_{V_{\max}}/r_{W_{\max}} \approx 1.37 \quad (4)$$

is constant over the entire section, as is the degree of twist of the jet (the ratio of axial velocity to tangential velocity):

$$V_{\max}/W_{\max} = \text{const}, \quad (5)$$

the tangential velocity maximum meanwhile being nearer to the jet axis for any ratio  $G_a/G_q$ . beyond the initial section at the distance  $X = 40$  mm the ratio (4) is equal to 1 and subsequently continues to decrease. The carrier flow is curved on the initial section and, thus, the liquid particles within the flow move in a curved path, leading to their collision with one another.

TABLE 1. Thickness of the External "Boundary" Layer

$X, \text{ mm}$	5	10	20	30	40	60	80	100	120	160	200	250
$r, \text{ mm}$	7	11	15	21	26	42	55	64	74	90	202	121
$b, \text{ mm}$	2	2,0	2,0	2,4	3,6	4,4	5,2	6	6,8	8,4	10	12
$b_e, \text{ mm}$	2,2	2,3	2,4	2,3	2,7	4	5,2	6	7,2	8,5	10,6	11

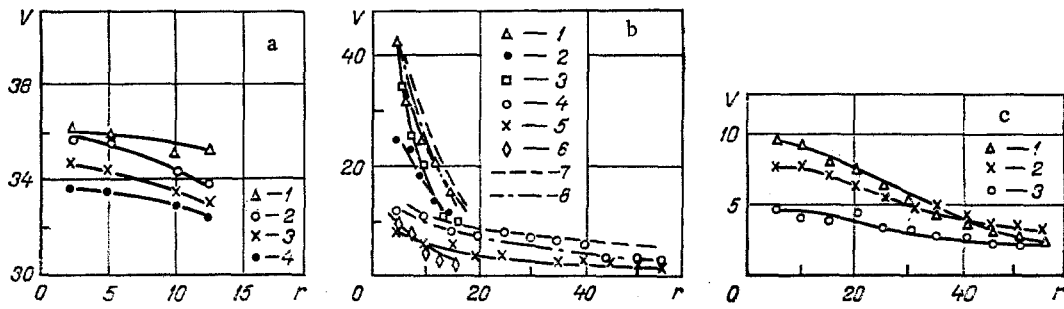


Fig. 2. Dependence of drop velocity on jet radius in different sections X: a)  $d = 30 \mu\text{m}$  (1 -  $X = 5 \text{ mm}$ ; 2 - 10; 3 - 20; 4 - 30); b)  $X = 40 \text{ mm}$  (1 - air velocity; 2 - drop velocity,  $d = 40\text{-}60 \mu\text{m}$ ; 3 - drop velocity,  $d = 100 \mu\text{m}$ );  $X = 200 \text{ mm}$  (4 - air velocity; 5 - drop velocity,  $d = 40\text{-}60 \mu\text{m}$ ; 6 - drop velocity,  $d = 100 \mu\text{m}$ ); 7) Abramovich model; 8) Laats model; c)  $X = 200 \text{ mm}$  (1 - air velocity; 2 - particle velocity,  $d = 20 \mu\text{m}$ ; 3 - particle velocity,  $d = 100 \mu\text{m}$ ).  $V$ , m/sec;  $r$ , mm.

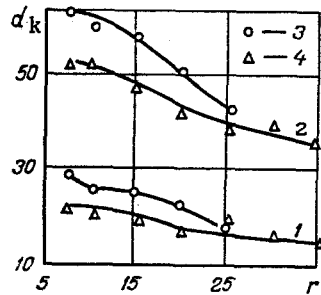


Fig. 3

Fig. 3. Distribution of drop diameter over the jet radius at different stations with different ratios  $G_a/G_q$ : 1)  $G_a/G_q = 3.9 \cdot 10^3$ ; 2)  $2.4 \cdot 10^3$ ; 3)  $X = 50 \text{ mm}$ ; 4) 200;  $d_k$ ,  $\mu\text{m}$ ;  $r$ , mm.

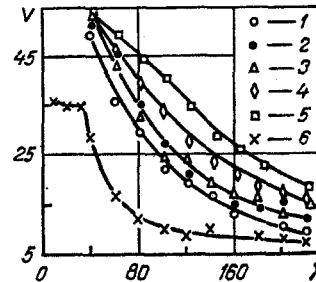


Fig. 4

Fig. 4. Distribution of velocity of air with particles on the jet axis with different relative concentrations  $\alpha$ : 1) air velocity; 2) drop velocity,  $d = 20 \mu\text{m}$  at  $\alpha = 0.11$ ; 3) particle velocity,  $d = 100 \mu\text{m}$  at  $\alpha = 0.11$ ; 4) particle velocity,  $d = 20 \mu\text{m}$  at  $\alpha = 0.25$ ; 5) drop velocity,  $d = 20 \mu\text{m}$  at  $\alpha = 0.35$ ; 6) velocity of kaolin particles,  $d = 50 \mu\text{m}$  at  $\alpha = 0.22$ .  $X$ ,  $r$ ,  $b$ ,  $b_e$ , mm.

According to the theory of disintegration of a stream into drops, the Weber criterion at which a stream is broken up lies within the following interval:  $1.3 \leq We \leq 7$ . After breakdown of the jet, the Weber criterion

$$We = \frac{\rho d V^2}{\sigma} \leq 1. \quad (6)$$

The results of the experiment (Fig. 3) showed that breakup of the drops also occurs beyond the limits of the jet disintegration region. Meanwhile, it was noted that the higher the ratio  $G_a/G_q$ , the smaller the difference in drop dimensions in different sections. No difference was seen at the maximum ratio  $G_a/G_q = 5.5 \cdot 10^{-3}$  seen in our experiment. This is explained by the fact that at ratios  $G_a/G_q = 1 \cdot 10^3\text{-}2.4 \cdot 10^3$  coarse drops from 100 to 60  $\mu\text{m}$  in diameter are formed, and these drops collide and are broken up as they move in the jet. At the ratio  $G_a/G_q = 5.5 \cdot 10^3$ , the dimensions of the drops formed are such that surface tension prevents breakup of drops as a result of collision. To check this proposition, we conducted a model experiment in which we determined the velocities of particles of different diameters introduced into a jet spray. As the disperse phase we used solid particles of kaolin 5 and 20  $\mu\text{m}$  in diameter and 100- $\mu\text{m}$ -diam. particles of dry milk powder. It is apparent from the measurements of the velocities of individual particles shown in Fig. 2c and Fig. 3 that there is a 25 m/sec difference in the velocities of the 20- and 100- $\mu\text{m}$ -diam. drops at the distance  $X = 40 \text{ mm}$  and that this difference decreases to 2 m/sec at the distance of 200 mm. Thus, the process of drop breakup and the formation of secondary drops occurs most intensively immedi-

ately after the constant-velocity zone. At distances greater than 200 mm from the nozzle edge, the velocities of drops of different sizes differ little, the drop paths are almost parallel, and the probability of their collision decreases. When collision does occur, the interaction forces are too small to result in the formation of secondary drops. It should be pointed out that the velocity of the 20- and 100- $\mu\text{m}$ -diam. solid particles added to the flow was somewhat greater than the axial velocity of the flow itself. This is due to the fact that the solid particles pass through a high-velocity zone on their way to the flow axis and thus acquire a greater speed. The coarser particles accelerate slowly but also decelerate slowly. Figure 2b shows results of measurement of the velocities of the particles in the 3-phase flow and compares them with theoretical results obtained by the Abramovich [10] and Latts [11] formulas. The presence of solid particles in the liquid jet spray has a significant effect on its hydrodynamics, particularly if the concentration of particles introduced increases (Fig. 4). In this case, the axial velocity of the carrier flow decreases, while the velocity of the introduced disperse phase increases as a result of transfer of energy from the air to the disperse phase.

#### NOTATION

R, particle radius; V, velocity; n, nonuniformity factor;  $b_n$ , thickness of boundary layer in the initial section at the nozzle edge; X, distance along jet axis;  $V_0$ , mean-flow-rate discharge velocity of jet;  $V_{0m}$ , velocity on axis of nozzle edge;  $\rho$ , density of liquid;  $\sigma$ , surface tension; d, particle diameter;  $\rho$ , density of the material; r, distance over radius of jet spray; W, tangential velocity.

#### LITERATURE CITED

1. B. S. Rinkevichnyus, "Doppler method of measuring local velocities by means of lasers," *Usp. Fiz. Nauk*, 3, No. 2, 305-330 (1973).
2. B. S. Rinkevichyus and G. M. Yanina, "Determination of the dimensions of optical discontinuities by means of a Doppler velocity meter," *Tr. Mosk. Energ. Inst., Fiz.*, 94, 76-81 (1971).
3. I. V. Khodan, S. A. Pylev, and V. Liliemblyum, "Study of the velocity field of a gas-liquid flow in an inclined column by means of a laser-Doppler velocity meter," in: *Heat and Mass Transfer: Physical Principles and Methods of Investigation [in Russian]*, ITMO, Minsk (1980), pp. 32-34.
4. V. Ya. Borovoi et al., "Visualization of three-dimensional flow about models by means of a 'laser knife'," *Uch. Zap. TsAGI*, 4, No. 5, 42-49 (1973).
5. V. A. Borodulya, E. Varela Bel'ov, A. Zh. Greben'kov, et al., "Study of the hydrodynamics of sprayers by means of a laser-Doppler velocity meter," *Materials of an International School-Seminar. Current Experimental Methods of Studying Heat and Mass Transfer [in Russian]*, Vol. 2, ITMO, Minsk (1981), pp. 64-73.
6. A. P. Alkhimov and A. N. Papyrin, "An application of the method of high-speed laser visualization of the study of two-phase flows," *Tr. TsAGI*, No. 1975, 175-181 (1976).
7. B. S. Rinkevichyus and G. M. Yanina, "Doppler method of studying two-phase flows," in: *Turbulent Flows [in Russian]*, Izd. Akad. Nauk Estonian SSR, Tallin (1976), pp. 162-168.
8. A. P. Alkhimov, A. N. Papyrin, A. L. Peredin, and R. I. Soloukhin, "Experimental study of the effect of particle lag in a supersonic gas flow," *Zh. Prikl. Mekh. Tekh. Fiz.*, No. 4, 80-88 (1977).
9. V. A. Dvoinishnikov, M. A. Laryushkin, and V. P. Knyaz'kov, "Effect of nonuniform initial velocity profile on the development of an axisymmetric free jet," *Tr. Mosk. Energ. Inst., Probl. Parogeneratorostr.*, No. 330, 100-104 (1977).
10. G. N. Abramovich, V. I. Bazhanov, and T. A. Girshovich, "Turbulent jet with heavy impurities," *Izv. Akad. Nauk SSSR, Mekh. Zhidk. Gaza*, No. 6, 41-49 (1972).
11. V. Vanatoa, M. Laats, A. Kartushinskii, and F. Frishman, "Integral method of calculating a two-phase nonequilibrium jet," *Izv. Akad. Nauk Est. SSR, Fiz. Mat.*, 26, No. 4, 445-449 (1977).